Cumhuriyet Sci. J., 45(4) (2024) 777-788
DOI: https://doi.org/10.17776/csj.1445761

Cumhuriyet Science Journal

| csj.cumhuriyet.edu.tr | Founded: 2002 ISSN: 2587-2680 e-ISSN: 2587-246X Publisher: Sivas Cumhuriyet University

New accurate conservative finite difference schemes for 1-D and 2-D Schrödinger-Boussinesq Equations

Ayhan Aydın [1,a,*], Taha Mohammed [2,3,b]

[1] Department of Mathematics, Faculty of Art and Science, Atilim University, 08830, Incek, Ankara, Türkiye.
[2] Graduate School of Natural and Applied Sciences, Atilim University, 08830 , Incek, Ankara, Türkiye.
[3] Al-Farahidi University, Department of Business Management, Faculty of Administration and Economics, Baghdad, Iraq.
*Corresponding author

Research Article

History
Received: 02/03/2024
Accepted: 12/12/2024

ABSTRACT

In this paper, first-order and second-order accurate structure-preserving finite difference schemes are proposed for solving the Schrödinger- Boussinesq equations. The conservation of the discrete energy and mass of the present schemes are analytically proved. Numerical experiments are given to support the theoretical results. Numerical examples show the efficiency of the proposed scheme and the correction of the theoretical proofs.

Keywords: Conservative numerical methods, Partitioned average vector field method, Soliton solution, Schrödinger- Boussinesq equations.

[a] ayhan.aydin@atilim.edu.tr https://orcid.org/0000-0002-0837-9364 [b] taha.y.mohammed@gmail.com https://orcid.org/0000-0002-5679-9195

Introduction

The coupled partial differential equations such as Schrödinger-KDV equations [1], N-coupled nonlinear Schrödinger equations [2], and the coupled Gross-Pitaevskii equations [3] play a crucial role in applied mathematics, engineering, and physics, many of which are the models of various nonlinear phenomena. In this paper, we consider the coupled nonlinear Schrödinger-Boussinesq (CNSB) equations

$$\begin{aligned} &iu_t = -\gamma\Delta u + \xi uv, \quad i^2 = -1, \\ &v_t = \Delta\phi, \\ &\phi_t = -\alpha\Delta v + v + f(v) + \omega|u|^2 \end{aligned} \tag{1}$$

where the complex function $u(\boldsymbol{x},t)$ describes the electrical field of Langmuir oscillations, real valued function $v(\boldsymbol{x},t)$ represents low frequency density perturbation, $\boldsymbol{x} = (x_1,\dots,x_d)^T \in \Omega \subset \mathbb{R}^d$, $t = [0,T]$.

The parameters γ,ξ,ω and $\alpha > 0$ are constant, and $f(x)$ is sufficiently smooth real function with $f(0) = 0$. The equations (1) describe a coupling motion of acoustic and optical wave [4] and the dynamics behavior of Langmuir soliton formation [5]. We study the equations (1) with initial conditions

$$u(\boldsymbol{x},0) = u_0(x),\ v(\boldsymbol{x},0) = v_0(\boldsymbol{x}),\ \phi(\boldsymbol{x},0) = \phi_0(\boldsymbol{x}), \boldsymbol{x}\ \boldsymbol{\Omega} \tag{2}$$

and $(l_1,\dots,l_d)$- periodic boundary conditions

$$\begin{aligned} &u(\boldsymbol{x},t) = u(x_1 + l_1,\dots x_d,t),\dots, \\ &u(\boldsymbol{x},t) = u(x_1,\dots,x_d + l_d,t) \\ &v(\boldsymbol{x},t) = v(x_1 + l_1,\dots x_d,t),\dots, \\ &v(\boldsymbol{x},t) = v(x_1,\dots,x_d + l_d,t), \\ &\phi(\boldsymbol{x},t) = \phi(x_1 + l_1,\dots x_d,t),\dots, \\ &\phi(\boldsymbol{x},t) = \phi(x_1,\dots,x_d + l_d,t), \end{aligned} \tag{3}$$

,

which makes long time integration possible. The spatial domain Ω is truncated on a bounded interval in one dimension $(d = 1)$, a rectangle in two dimensions $(d = 2)$ or a box in three dimensions $(d = 3)$. One of the main properties of the periodic- initial- value problem (1)-(3) is conservation of mass (or the Langmuir plasmon number)

$$M(t) \coloneqq \int_\Omega |u(\boldsymbol{x},t)|^2\, d\boldsymbol{x} \equiv M(0) \tag{4}$$

and the total energy

$$\begin{aligned} E(t) \coloneqq \int_\Omega \Big(&\tfrac{2\gamma\omega}{\xi}|\nabla u|^2 + \alpha|\nabla v|^2 + |\nabla\phi|^2 + v^2 + \\ &2F(v) + 2\omega v|u|^2\ \Big)\, d\boldsymbol{x} \equiv E(0) \end{aligned} \tag{5}$$

where $F(v)$ is the primitive function of $f(v)$. The CNSB equations (1) are conservative systems. Therefore, proper discretization is required to reflect the conservation properties (4)-(5). In general, conservative numerical scheme exhibits better numerical performance on long time integration than a nonconservative one [12].

The CNSB equations (1) have been solved numerically by several authors. In [6], a multi-symplectic Hamiltonian formulation has been presented for the CNSB. Liao et al. proposed two conserved compact finite difference schemes for solving the nonlinear CNSB equations [20]. Bai et al. proposed a quadratic B-spline finite element scheme for the CNSB equations [7]. Zhang et al. studied the implicit conservative difference scheme and obtained an optimal error estimate [8]. Bai et al. studied the CNSB equations by the time-splitting Fourier spectral method [10]. All these numerical methods for the CNSB equations are obtained by constructing the

appropriate discretization. However, these methods for high dimensional CNSB equations $(d \geq 2)$ are time-consuming and difficult since the resulting schemes are fully coupled and nonlinearly implicit. Few numerical methods are available in the literature for the numerical solution of multi-dimensional $(d \geq 2)$ CNSB equations. Liao et al. proposed a time-splitting exponential wave integrator method based on Gautschi-type quadrature and Fourier pseudo-spectral discretization for solving Boussinesq-like equation and then presented the time-splitting Fourier spectral discretization for Schrödinger-like equation [11]. Two efficient compact finite difference schemes are introduced in [25] and [26]. By a combination of the Crank-Nicolson method and Leap-Frog scheme for temporal discretization and second-order centered difference scheme for spatial approximations, a linear Energy and Mass Preserving Finite Difference Method (EMP-FDM) is devised for 1D CSBEs in [27]. Cai et al. [19] developed second and fourth-order energy-preserving wavelet collocation schemes for CNSB equations based on the Hamiltonian structure and composition technique. The proposed method is energy-preserving but does not preserve mass. In many cases, the conservation of energy is more important than the conservation of mass. Recently, extensive structure-preserving numerical methods have been carried out for the numerical solution of dispersive/dissipative partial differential equations in the literature (see [28] and references therein). For instance, a fourth-order compact and energy-conservative difference scheme is proposed for solving the two-dimensional nonlinear Schrödinger equation, and convergence analysis of the method has been carried out in [29]. The numerical study of fractional differential equations is also a challenging problem for many authors (see [30] and reference therein). For instance, The Schrodinger equation with the variable-order fractional operator has been solved numerically in [31]. In that study, an implicit fully discrete continuous Galerkin finite element method was developed to tackle this equation while the fractional operator was expressed with a nonsingular Mittag-Leffler kernel. Quispel et al. [13] developed the so-called Average Vector Field (AVF) method for ordinary differential equations (ODEs) which is energy preserving for the Hamiltonian vector field. Under most circumstances, the second-order AVF method yields a fully implicit numerical scheme that requires a nonlinear solver such as Newton's iteration. Cai et al. [16] developed a more efficient AVF-based method and call this method a partitioned AVF (PAVF) method which can also automatically preserve arbitrary Hamiltonian energy of the Hamiltonian system. In [24] an explicit scheme has been developed for the Zakharov equation using the PAVF method. The main purpose of this study is to develop a new energy-preserving scheme for the CNSB equations (1) based on the PAVF method. Firstly, the equations (1) are written in an infinite Hamiltonian form. Then, the second-order central difference is employed for the spatial discretization to cast the CNSB equations (1) into a finite-dimensional Hamiltonian equation. We use the PAVF method for time integration to develop the energy-preserving scheme. The proposed scheme is semi-implicit which has a significant advantage over the AVF method. In conjunction with the adjoint method, we further present the PAVF composition (PAVF-C) method and the PAVF plus (PAVF-P) method for the CNSB equations (1).

Construction of a finite difference scheme

Many evolution PDEs can be written as an infinite-dimensional Hamiltonian system of the form [23]

$$\frac{dz}{dt} = \mathcal{D}\frac{\delta \mathcal{H}}{\delta z} \tag{6}$$

where $z = z(x,t) \in \mathbb{R}^d \times \mathbb{R}$ and $\mathcal{D}$ is a constant linear differential operator. For example, if $d = 1$ and $z(x,t)$ belongs to the Hilbert space $L^2(\Omega)$, the Hamiltonian $\mathcal{H}$ and the variational derivative is

$$\mathcal{H}(z) = \int_\Omega H(x, z, z_x, z_{xx}, \dots)dx, \tag{7}$$

$$\frac{\delta \mathcal{H}}{\delta z} = \frac{\partial H}{\partial z} + \partial_x\left(\frac{\partial H}{\partial z_x}\right) - \partial_{xx}\left(\frac{\partial H}{\partial z_{xx}}\right) - \cdots \tag{8}$$

where $\Omega \subset \mathbb{R}$ and $z(x,t)$ satisfies homogenous or periodic boundary conditions. For two dimensions $d = 2$, i.e. $x = (x,y)^T, \Omega = [x_L, x_R] \times [y_L, y_R]$ the Hamiltonian $\mathcal{H}$ and the variational derivative is

$$\mathcal{H}(z) = \iint_\Omega H\big(x, y, z, z_x, z_y, z_{xx}, \dots\big)dxdy, \tag{9}$$

$$\frac{\delta \mathcal{H}}{\delta z} = \frac{\partial H}{\partial z} + \partial_x\left(\frac{\partial H}{\partial z_x}\right) + \partial_y\left(\frac{\partial H}{\partial z_y}\right) - \partial_{xx}\left(\frac{\partial H}{\partial z_{xx}}\right) - \cdots \tag{10}$$

By decomposing $u(x,t) = p(x,y,t) + iq(x,y,t)$ in real and imaginary components, the CNSB equations (1) in two space dimensions can be written as a first order system of equations

$$\begin{aligned} p_t &= -\gamma\big(q_{xx} + q_{yy}\big) + \xi q v \\ q_t &= \gamma\big(p_{xx} + p_{yy}\big) - \xi p v \\ v_t &= \phi_{xx} + \phi_{yy} \\ \phi_t &= v - \alpha\big(v_{xx} + v_{yy}\big) + f(v) + \omega(p^2 + q^2) \end{aligned} \tag{11}$$

which can be written as infinite-dimensional Hamiltonian system (6) with the state variable $z(t) = (p(x,y,t), q(x,y,t), v(x,y,t), \phi(x,y,t))^T$, the differential operator

$$\mathcal{D} = \begin{pmatrix} 0 & \xi/(4\omega) & 0 & 0 \\ -\xi/(4\omega) & 0 & 0 & 0 \\ 0 & 0 & 0 & -1/2 \\ 0 & 0 & 1/2 & 0 \end{pmatrix}$$

and the Hamiltonian

$$H(t) := \iint_\Omega \left(\frac{2\gamma\omega}{\xi} |\nabla u|^2 + \alpha |\nabla v|^2 + |\nabla \phi|^2 + v^2 + 2F(v) + 2\omega v |u|^2 \right) dx\, dy\,. \tag{12}$$

Remark: We can find that the Hamiltonian $H(t)$ is the total energy (5) of the system (1).

In the following sections, we propose a nonlinear two-level, conservative and second-order accurate finite difference scheme for the problem (1)-(3).

Spatial discretization

For simplicity of notations, we shall consider the CNSB system (1) in one space dimension. Extension to higher dimensions is straightforward. The domain $\{(x,t) | (x,t) \in \Omega \times [0,T]\}$ is discretized into grids by the set (x_j, t_n) of nodes, in which $x = x_L + jh$, $0 \le j \le N+1, t_n = n\tau, 0 \le n \le M$, where $h = (x_R - x_L)/N$, $\tau = T/M$, M and N are positive integers. Let p_j^n, q_j^n, v_j^n and ϕ_j^n be the approximations to $p(x,t)$, $q(x,t)$, $v(x,t)$ and $\phi(x,t)$ at the grid (x_j, t_n), respectively. For convenience, we introduce some notations:

$$\delta_t z_j^n = \frac{z_j^{n+1} - z_j^n}{\tau}, \quad \delta_x^+ z_j^n = \frac{z_{j+1}^n - z_j^n}{h}, \quad \delta_x^- z_j^n = \frac{z_j^n - z_{j-1}^n}{h}, \quad z_j^{n+\frac{1}{2}} = \frac{z_j^{n+1} + z_j^n}{2}$$
$$\delta_x^{+-} z_j^n = \delta_x^+ (\delta_x^- z_j^n) = \frac{z_{j+1}^n - 2z_j^n - z_{j-1}^n}{h^2}\,, \tag{13}$$

Discrete periodic boundary conditions are treated as

$$z_j = z_{N+j}, \quad j = \cdots, -2, -1, 0, 1, 2, \ldots$$

Consider the spatial discretization of the equations (11) in one space dimension

$$\begin{aligned} \frac{d}{dt} p_j &= -\gamma(\delta_x^{\pm} q_j) + \xi q_j v_j, \\ \frac{d}{dt} q_j &= \gamma(\delta_x^{+-} p_j) - \xi p_j v_j, \\ \frac{d}{dt} v_j &= \delta_x^{+-} \phi_j \quad , \\ \frac{d}{dt} \phi_j &= -\alpha(\delta_x^{+-} v_j) + v_j + f(v_j) + \omega(p_j^2 + q_j^2) \end{aligned} \tag{14}$$

where $j = 1, \ldots, N$. The system of equations (14) can be written as a finite-dimensional canonical Hamiltonian system

$$\frac{d}{dt} Z = \bar{\mathcal{D}} \nabla \bar{H}(Z) \tag{15}$$

where $Z = (p^T, q^T, v^T, \phi^T)^T, p, q, v, \phi \in \mathbb{R}^N$ with entries $p = (p_1, \ldots, p_N)^T, q = (q_1, \ldots, q_N)^T, v = (v_1, \ldots, v_N)^T, \phi = (\phi_1, \ldots, \phi_N)^T$, respectively,

$$\bar{\mathcal{D}} = \begin{pmatrix} 0 & \frac{\xi}{4\omega} I & 0 & 0 \\ -\frac{\xi}{4\omega} I & 0 & 0 & 0 \\ 0 & 0 & 0 & -\frac{1}{2} I \\ 0 & 0 & \frac{1}{2} I & 0 \end{pmatrix} \tag{16}$$

where $I = N \times N$ identity matrix, 0 is the $N \times N$ zero matrix and

$$\bar{H} = \sum_{i=1}^N \left(\frac{2\gamma\omega}{\xi} \left((\delta_x^+ p_j)^2 + (\delta_x^+ q_j)^2 \right) + \alpha (\delta_x^+ v_j)^2 + (\delta_x^+ \phi_j)^2 + v_j^2 + 2F(v_j) + 2\omega v_j |u_j|^2 \right) h. \tag{17}$$

Is the discrete Hamiltonian. The system (15) conserves the discrete Hamiltonian (17) in the sense that

$$\frac{d\bar{H}(Z(t))}{dt} = \nabla \bar{H}(Z(t)) \frac{dZ(t)}{dt} = \nabla \bar{H}(Z(t)) \bar{\mathcal{D}} \nabla \bar{H}(Z(t)) = 0 \tag{18}$$

due to the skew-symmetric property of the matrix $\bar{\mathcal{D}}$. Therefore, the flow of the semi-discrete system (15) preserves the Hamiltonian $\bar{H}(Z)$ exactly. The Hamiltonian system (15) also possesses symplecticity [21, 22]. The conservation of energy is as important as the conservation of symplectic structure in numerical simulations. Therefore, it is natural to

integrate (15) in time with a conservative method. In the following section, energy preserving PAVF methods have been developed for (15).

Temporal discretization

Here we briefly discuss the AVF and PAVF methods and their energy-preserving properties. We consider the Hamiltonian differential equation (15) with $Z = (a, b)^T$. The canonical Hamiltonian system (15) can be written as

$$\frac{d}{dt}\begin{pmatrix} a \\ b \end{pmatrix} = \bar{\mathcal{D}}\begin{pmatrix} \nabla_a \bar{H}(a,b) \\ \nabla_b \bar{H}(a,b) \end{pmatrix} \tag{19}$$

The energy preserving AVF integrator [13] for canonical Hamiltonian equation (19) is given by

$$\frac{1}{\tau}\begin{pmatrix} a^{n+1} + a^n \\ b^{n+1} + b^n \end{pmatrix} = \bar{\mathcal{D}}\begin{pmatrix} \int_0^1 \nabla_a \bar{H}(\xi a^{n+1} + (1-\xi)a^n, \xi b^{n+1} + (1-\xi)b^n)d\xi \\ \int_0^1 \nabla_b \bar{H}(\xi a^{n+1} + (1-\xi)a^n, \xi b^{n+1} + (1-\xi)b^n)d\xi \end{pmatrix} \tag{20}$$

Theorem 1. [14] The scheme (20) is energy preserving, which possesses the discrete energy i.e.

$$\bar{H}(a^n, b^n) = \bar{H}(a^{n-1}, b^{n-1}) = \cdots = \bar{H}(a^0, b^0) \tag{21}$$

Proof. Taking the scalar product on both sides of (20) with

$$\left(\int_0^1 \nabla_a \bar{H}(\xi a^{n+1} + (1-\xi)a^n, \xi b^{n+1} + (1-\xi)b^n)^T\, d\xi, \int_0^1 \nabla_b \bar{H}(\xi a^{n+1} + (1-\xi)a^n, \xi b^{n+1} + (1-\xi)b^n)^T d\xi\right)^T$$

using the Fundamental Theorem of Calculus and the skew-symmetry of $\bar{\mathcal{D}}$, we have

$$\frac{1}{\tau}\left(\bar{H}(a^{n+1}, b^{n+1}) - \bar{H}(a^n, b^n)\right) = 0$$

that is, the energy $\bar{H}$ is precisely conserved at every time step. This completes the proof.

For polynomial Hamiltonian, the integral can be evaluated exactly, and the implementation is comparable to that of implicit Runge-Kutta method such as the implicit mid-point rule. When Hamiltonian energy is a quadratic function, the resulting AVF scheme is linearly implicit and therefore can be efficiently solved. However, this is not the case to reflect the merit of the AVF method since any symplectic Runge-Kutta method can also achieve the energy conservation of the quadratic Hamiltonian [12]. Under most circumstances, the evaluation of the integration in (20) leads to nonlinear function of Z^{n+1} which further constitutes a fully implicit numerical scheme. The iterative processes are then inevitably required but this leads to an increase in computation complexity, especially for the application of Hamiltonian PDEs. Cai [16] et. al. defined the so-called PAVF method for the Hamiltonian system (19) which has a remarkable advantage over the AVF method (20). The one-step, first-order PAVF method for the Hamiltonian system (19) is written as

$$\frac{1}{\tau}\begin{pmatrix} a^{n+1} + a^n \\ b^{n+1} + b^n \end{pmatrix} = \bar{\mathcal{D}}\begin{pmatrix} \int_0^1 \nabla_a \bar{H}(\xi a^{n+1} + (1-\xi)a^n, b^n)d\xi \\ \int_0^1 \nabla_b \bar{H}(a^{n+1}, \xi b^{n+1} + (1-\xi)b^n)d\xi \end{pmatrix} \tag{22}$$

Theorem 2. [14] The scheme (22) is energy preserving in the sense that

$$\bar{H}(a^n, b^n) = \bar{H}(a^{n-1}, b^{n-1}) = \cdots = \bar{H}(a^0, b^0) \tag{23}$$

Proof. Taking the scalar product on both sides of (22) with

$$\left(\int_0^1 \nabla_a \bar{H}(\xi a^{n+1} + (1-\xi)a^n, b^n)d\xi\,, \int_0^1 \nabla_b \bar{H}(a^{n+1}, \xi b^{n+1} + (1-\xi)b^n)d\xi\right)^T$$

right-hand side of (22) vanishes by the skew-symmetry of $\bar{\mathcal{D}}$. The left-hand side of (22) can be written as

$$\frac{1}{\tau}\left(\int_0^1 \nabla_a \bar{H}(\xi a^{n+1} + (1-\xi)a^n, b^n)d\xi\right)(a^{n+1} + a^n) + \frac{1}{\tau}\left(\int_0^1 \nabla_b \bar{H}(a^{n+1}, \xi b^{n+1} + (1-\xi)b^n)d\xi\right)(b^{n+1} + b^n) = 0$$

which can be written as

$$\frac{1}{\tau}\int_0^1 \frac{d}{d\xi}[\bar{H}(\xi a^{n+1} + (1-\xi)a^n, b^n) + \bar{H}(a^{n+1}, \xi b^{n+1} + (1-\xi)b^n)]d\xi = 0.$$

Using the Fundamental Theorem of Calculus, we have

$\frac{1}{\tau}[\bar{H}(a^{n+1},b^n)-\bar{H}(a^n,b^n)+\bar{H}(a^{n+1},b^{n+1})-\bar{H}(a^{n+1},b^n)]=0$ i.e. $\frac{1}{\tau}[\bar{H}(a^{n+1},b^{n+1})-\bar{H}(a^n,b^n)]=0.$

This completes the proof.

Definition 1. [12] The adjoint φ_τ^* of the method φ_τ is the inverse map of the original method with reversed time step $-\tau$.

The adjoint of the explicit Euler method is the implicit Euler method. The adjoint method of the implicit mid-point rule is the implicit mid-point rule itself, that is the implicit mid-point rule is symmetric. Accordingly, reversing the path order in (22), the adjoint method of the PAVF method (22) is written as [16]

$$\frac{1}{\tau}\begin{pmatrix}a^{n+1}+a^n\\ b^{n+1}+b^n\end{pmatrix}=J\begin{pmatrix}\int_0^1\nabla_a\bar{H}(\xi a^{n+1}+(1-\xi)a^n,b^{n+1})d\xi\\ \int_0^1\nabla_b\bar{H}(a^n,\xi b^{n+1}+(1-\xi)b^n)d\xi\end{pmatrix} \tag{24}$$

The adjoint method has the same order as the original method. In the following, we consider the composition of the PAVF method (22) and the adjoint method (24) with the same step size. This allows an order increase for the old order method. If Φ_τ is the method (22) and Φ_τ^* is the adjoint method (24) then the composition method [16]

$$\hat{\Phi}_h=\Phi_{\frac{\tau}{2}}\circ\Phi_{\frac{\tau}{2}}^* \tag{25}$$

is the second order method and conserves the Hamiltonian exactly. Analogously, taking the average of the Φ_τ and Φ_τ^*, we can write the plus method [16]

$$\hat{\Phi}_h=\frac{1}{2}(\Phi_\tau+\Phi_\tau^*) \tag{26}$$

Average Vector Field for CNSB Equations

We first present the conventional second-order AVF method (20) for CNSB equations (1) [18]. To obtain the AVF integrator, we apply the AVF method to time integration for the semi-discrete system (15) as follows.

$$\begin{aligned}
\delta_t\left(p_j^n\right) &= -\gamma\delta_x^{+-}\left(q_j^{n+\frac{1}{2}}\right)+\xi\left(\tfrac{1}{3}q_j^{n+1}v_j^{n+1}+\tfrac{1}{6}q_j^{n+1}v_j^n+\tfrac{1}{6}q_j^nv_j^{n+1}+\tfrac{1}{3}q_j^nv_j^n\right),\\
\delta_t\left(q_j^n\right) &= \gamma\delta_x^{+-}\left(p_j^{n+1/2}\right)-\xi\left(\tfrac{1}{3}p_j^{n+1}v_j^{n+1}+\tfrac{1}{6}p_j^{n+1}v_j^n+\tfrac{1}{6}p_j^nv_j^{n+1}+\tfrac{1}{3}p_j^nv_j^n\right),\\
\delta_t\left(v_j^n\right) &= \delta_x^{+-}\left(\phi_j^{n+1/2}\right)\\
\delta_t\left(\phi_j^n\right) &= -\alpha\delta_x^{+-}\left(v_j^{n+1/2}\right)+v_j^{n+1/2}+\tilde{f}\left(v_j^{n+1},v_j^n\right)+\frac{\omega}{3}\begin{pmatrix}\left(p_j^{n+1}\right)^2+p_j^{n+1}p_j^n+\left(p_j^n\right)^2\\ +\left(q_j^{n+1}\right)^2+q_j^{n+1}q_j^n+\left(q_j^n\right)^2\end{pmatrix}.
\end{aligned} \tag{27}$$

where $\tilde{f}\left(v_j^{n+1},v_j^n\right)=\int_0^1 f(\xi v_j^{n+1}+(1-\xi)v_j^n)d\xi$. We see that the scheme (27) is fully implicit, which requires a time consuming iterative method such as Newton-Raphson method. Now, we propose a more efficient energy-preserving method for CNSB equations (1).

Partitioned Average Vector Field for CNSB Equations

Upon applying the PAVF method (22) to the semi-discrete system (15), we obtain

$$\begin{aligned}
\delta_t\left(p_j^n\right) &= -\gamma\delta_x^{\pm}\left(q_j^{n+\frac{1}{2}}\right)+\tfrac{\xi}{2}\left(q_j^{n+1}v_j^n+q_j^nv_j^n\right),\\
\delta_t\left(q_j^n\right) &= \gamma\delta_x^{+-}\left(p_j^{n+1/2}\right)-\frac{\xi}{2}\left(p_j^{n+1}v_j^n+p_j^nv_j^n\right),\\
\delta_t\left(v_j^n\right) &= \delta_x^{+-}\left(\phi_j^{n+1/2}\right)\\
\delta_t\left(\phi_j^n\right) &= -\alpha\delta_x^{+-}\left(v_j^{n+\frac{1}{2}}\right)+v_j^{n+1/2}+\tilde{f}\left(v_j^{n+1},v_j^n\right)+\omega\left((p_j^{n+1})^2+(q_j^{n+1})^2\right)
\end{aligned} \tag{28}$$

The PAVF method (28) is simpler than the AVF method (27). The first two equations of (28) are linearly implicit according to the variables p^{n+1} and q^{n+1}. Once the values p_j^n, q_j^n, v_j^n and ϕ_j^n are known, the values p^{n+1} and q^{n+1} can be solved from the first two equations of (28) and substituted into the last two equations. Then the values ϕ_j^{n+1} and v_j^{n+1} can be solved from the last two equations by using an iterative method such as Newton's method. Although the PAVF method (28) for the CNSB is semi-implicit, the AVF method (27) is fully implicit which requires more cost per time step than PAVF method (28).

Remark: On the contrary to the semi-implicit structure of the PAVF method (28) for CNSB equations, Cai et. al. [16] have constructed the PAVF method to nonlinear Klien-Gordon-Schrödinger equations that requires to solve two sets of linear algebraic equations.

In addition, to the conservation of energy, the conservation of mass (4), which is quadratic invariant, also plays an important role in physics. Therefore, it is natural to discuss the mass conservation of the method (28).

Theorem 1. The difference scheme (28) is conservative, that is the mass (4) is conserved in the sense

$$M^n = \sum_{k=1}^{N}((p_k^n)^2 + (q_k^n)^2)h = M^{n-1} = \cdots = M^0, \tag{29}$$

where $M^n = M(p^n, q^n)$.

Proof. Multiplying both sides of the first line of equation (28) with $(p_j^{n+1} + p_j^n)^T$ yields

$$\frac{1}{\tau}\left(p_j^{n+1} + p_j^n\right)^T\left(p_j^{n+1} - p_j^n\right) = \left(p_j^{n+1} + p_j^n\right)^T\left(-\gamma\delta_x^{+-}q_j^n + \frac{1}{2}(q_j^{n+1}v_j^n + q_j^n v_j^n)\right) \tag{30}$$

Multiplying both sides of the second line of equation (28) with $(q_j^{n+1} + q_j^n)^T$ yields

$$\frac{1}{\tau}\left(q_j^{n+1} + q_j^n\right)^T\left(q_j^{n+1} - q_j^n\right) = \left(q_j^{n+1} + q_j^n\right)^T\left(\gamma\delta_x^{+-}p_j^n - \frac{1}{2}(p_j^{n+1}v_j^n + p_j^n v_j^n)\right). \tag{31}$$

Adding (30) to (31), we have

$$\frac{1}{\tau}\sum_{i=1}^{N}\left(\left(p_j^{n+1}\right)^2 + \left(q_j^{n+1}\right)^2\right) = \frac{1}{\tau}\sum_{i=1}^{N}\left(\left(p_j^n\right)^2 + \left(q_j^n\right)^2\right)$$

which completes the proof.

The adjoint PAVF method of the scheme (27) is given as

$$\begin{aligned}
\delta_t\left(p_j^n\right) &= -\gamma\delta_x^{+-}\left(q_j^{n+\frac{1}{2}}\right) + \frac{\xi}{2}\left(q_j^{n+1}v_j^{n+1} + q_j^n v_j^{n+1}\right),\\
\delta_t\left(q_j^n\right) &= \gamma\delta_x^{+-}\left(p_j^{n+1/2}\right) - \frac{\xi}{2}\left(p_j^{n+1}v_j^{n+1} + p_j^n v_j^{n+1}\right),\\
\delta_t\left(v_j^n\right) &= \delta_x^{+-}\left(\phi_j^{n+1/2}\right)\\
\delta_t\left(\phi_j^n\right)_t &= -\alpha\delta_x^{+-}\left(v_j^{n+1/2}\right) + v_j^{n+1/2} + \tilde{f}\left(v_j^{n+1}, v_j^n\right) + \omega\left((p_j^n)^2 + (q_j^n)^2\right).
\end{aligned} \tag{32}$$

We can see that the adjoint scheme (32) is semi-implicit due to the nonlinear term $\tilde{f}\left(v_j^{n+1}, v_j^n\right)$. The values v_j^{n+1} and ϕ_j^{n+1} can be solved from the last two nonlinear equations of (32) using an iterative method. Then v_j^{n+1} and ϕ_j^{n+1} can be substituted into the first two equations of (32) and p_j^{n+1} and q_j^{n+1} can be obtained. Using the PAVF method (28) with the adjoint method (32), we can write the energy-preserving composition (PAVF-C) method (25) as follows:

$$\begin{aligned}
\frac{2}{\tau}\left(p_j^* - p_j^n\right) &= -\gamma\delta_x^{+-}(q_j^* + q_j^n) + \xi(q_j^* v_j^n + q_j^n v_j^n)\\
\frac{2}{\tau}\left(q_j^* - q_j^n\right) &= \gamma\delta_x^{+-}\left(p_j^* + p_j^n\right) - \xi(p_j^* v_j^n + p_j^n v_j^n)\\
\frac{2}{\tau}\left(v_j^* - v_j^n\right) &= \delta_x^{+-}(\phi_j^* + \phi_j^n)\\
\frac{2}{\tau}\left(\phi_j^* - \phi_j^n\right) &= -\alpha\delta_x^{+-}\left(v_j^* + v_j^n\right) + \left(v_j^* + v_j^n\right) + 2\tilde{f}\left(v_j^*, v_j^n\right) + 2\omega\left(\left(p_j^*\right)^2 + \left(q_j^*\right)^2\right)\\
\frac{2}{\tau}\left(p_j^{n+1} - p_j^*\right) &= -\gamma\delta_x^{+-}(q_j^{n+1} + q_j^*) + \xi(q_j^{n+1}v_j^{n+1} + q_j^* v_j^{n+1})\\
\frac{2}{\tau}\left(q_j^{n+1} - q_j^*\right) &= \delta_x^{+-}\left(p_j^{n+1} + p_j^*\right) - \xi(p_j^{n+1}v_j^{n+1} + p_j^* v_j^{n+1})\\
\frac{2}{\tau}(v^{n+1} - v^*) &= \delta_x^{+-}(\phi_j^{n+1} + \phi_j^*)\\
\frac{2}{\tau}(\phi^{n+1} - \phi^*) &= -\alpha\delta_x^{+-}\left(v_j^{n+1} + v_j^*\right) + \left(v_j^{n+1} + v_j^*\right) + 2\tilde{f}\left(v_j^{n+1}, v_j^*\right) + 2\omega\left(\left(p_j^*\right)^2 + \left(q_j^*\right)^2\right)
\end{aligned} \tag{33}$$

We can see that the PAVF-C method (33) inherits the semi-implicit property. If the values p_j^n, q_j^n, v_j^n and ϕ_j^n are known, the values p_j^* and q_j^* can be solved from the first two equations of (33) and substituted into the third and fourth equations which are nonlinear in terms of the unknowns ϕ_j^* and v_j^*. Thus, ϕ_j^* and v_j^* can be obtained by using an iterative method. Here Newton's method is used as a nonlinear solver. Then, p_j^*, q_j^*, v_j^* and ϕ_j^* can be substituted into the last two equations in (33) and ϕ_j^{n+1} and v_j^{n+1} can be obtained by using Newton's method. Finally, ϕ_j^{n+1} and v_j^{n+1} can be substituted into the fifth and sixth equations and p_j^{n+1} and q_j^{n+1} can be obtained by using the semi-implicit property of these two equations.

With the adjoint scheme (32), we can write down the corresponding plus scheme (PAVF-P)

$$\delta_t\left(p_j^n\right) = -\gamma\delta_x^{+-}\left(q_j^n\right) - \frac{\xi}{4}\left(q_j^{n+1}v_j^n + q_j^n v_j^n + q_j^{n+1}v_j^{n+1} + q_j^n v_j^{n+1}\right)$$

$$\begin{aligned}\delta_t\left(q_j^n\right) &= \gamma\delta_x^{+-}\left(p_j^n\right) - \frac{\xi}{4}\left(p_j^{n+1}v_j^n + p_j^n v_j^n + p_j^{n+1}v_j^{n+1} + p_j^n v_j^{n+1}\right),\\ \delta_t\left(v_j^n\right) &= \delta_x^{+-}\left(\phi_j^n\right),\\ \delta_t\left(\phi_j^n\right) &= -\alpha\delta_x^{+-}\left(v_j^n\right) + v_j^{n+1/2} + \tilde{f}\left(v_j^{n+1}, v_j^n\right) + \frac{\omega}{2}\left((p_j^{n+1})^2 + (q_j^{n+1})^2 + (p_j^n)^2 + (q_j^n)^2\right)\end{aligned} \tag{34}$$

The scheme (34) is implicit and nonlinear. To obtain the numerical solution $p_j^{n+1}, q_j^{n+1}, v_j^{n+1}$ and ϕ_j^{n+1}in (34), we need an iterative algorithm which increases the computational time. Here Newton's method is used as a nonlinear solver.

Numerical Results

In this section, we present some numerical experiments to verify the theoretical results and to demonstrate the effectiveness of the conservative schemes (28), (33), (34). $L_\infty^n(\tau)$ and $L_2^n(\tau)$ errors for temporal accuracy is defined by

$$L_\infty^n = \max_{1\le j\le N}\{|u(x_j,t_n) - u_j^n| + |v(x_j,t_n) - v_j^n|\},$$

$$L_2^n = \left(h\sum_{j=1}^N |u(x_j,t_n) - u_j^n|^2\right)^{1/2} + \left(h\sum_{j=1}^N |v(x_j,t_n) - v_j^n|^2\right)^{1/2} \tag{35}$$

L_∞^j and L_2^j errors for spatial accuracy can be defined analogously. The preservation of the energy and the mass are monitored by the relative errors

$$GE = \frac{|H^n - H^0|}{|H^0|}, \qquad GM = \frac{|M^n - M^0|}{|M^0|}$$

where

$$H^n = \sum_{i=1}^N \left(\frac{2\gamma\omega}{\xi}\left((\delta_x^+ p_j^n)^2 + (\delta_x^+ q_j^n)^2\right) + \alpha(\delta_x^+ v_j^n)^2 + (\delta_x^+\phi_j^n)^2 + \left(v_j^n\right)^2 + 2F\left(v_j^n\right) + 2\omega v_j^n|u_j^n|^2\right)h.$$

denotes the discrete Hamiltonian corresponding to (17), and M^n is the mass (29) evaluated at $t = t^n$. The rate of convergence in time discretization is obtained by using

$$order \approx \log(L(\tau_1)/L(\tau_2))/\log(\tau_1/\tau_2)$$

where L represents $L_\infty^n(\tau)$ and $L_2^n(\tau)$ errors at the time steps τ_1 and τ_2. The rate of convergence in space discretization can be defined analogously. To demonstrate the long-time behavior of the energy-preserving schemes, we take periodic boundary conditions. For simplicity, we present the wave profiles of the PAVF scheme (28) in all computations, since the other schemes AVF (27), PAVF-C (33), and PAVF-P (34) produce the same profile.

One-dimensional CSB equation

In this section, we report some numerical results to exhibit the performance of the schemes (28), (33) and (34) and verify the energy and the mass conservations. Performance at the PAVF schemes (28), (33) and (34) are compared with the fully implicit AVF scheme (27) [18]. An analytical solution has been given in [17].

$$\begin{aligned}u(x,t) &= \frac{9}{10}\operatorname{sech}^2\left(\frac{\sqrt{15}}{10}\left(x - \frac{\sqrt{10}}{5}t\right)\right) exp\left(i\left(\frac{\sqrt{10}}{10}x + \frac{1}{2}t\right)\right),\\ v(x,t) &= \frac{9}{10}\operatorname{sech}^2\left(\frac{\sqrt{15}}{10}\left(x - \frac{\sqrt{10}}{5}t\right)\right),\\ v_t(x,t) &= \frac{9}{10}\operatorname{sech}^2\left(\frac{\sqrt{15}}{10}\left(x - \frac{\sqrt{10}}{5}t\right)\right)\tanh\left(\frac{\sqrt{15}}{10}\left(x - \frac{\sqrt{10}}{5}t\right)\right),\end{aligned} \tag{36}$$

Accuracy test: First, the correctness of the numerical schemes is examined. The spatial domain has been chosen large enough that solitary wave propagation does not affect the propagation of the wave. The initial conditions are taken from the exact solution (36).

$$u(x,0) = u_0(x),\ v(x,0) = v_0(x),\ v_t(x,0) = v_{t,0}(x), \tag{37}$$

Table 1 represents L_∞^j and L_2^j errors and convergence order in space. We note that all methods are both of second order in space.

Table 1. The L_∞^j and L_2^j errors and convergence orders in space of the proposed methods with $M = 4000$, and $-16 \le x \le 16$ at $t = 1$.

		h	0.5	0.25	0.125
AVF [18]	L_∞^j	Error	1.174×10^{-2}	3.014×10^{-3}	7.508×10^{-4}
		Order	/	1.96	2.00
	L_2^j	Error	1.739×10^{-2}	4.371×10^{-3}	1.094×10^{-4}
		order	/	1.99	2.00
PAVF	L_2^j	Error	1.175×10^{-2}	3.030×10^{-3}	7.687×10^{-4}
		Order	/	1.95	2.00
	L_2^j	Error	1.741×10^{-2}	4.392×10^{-3}	1.101×10^{-4}
		order	/	1.99	2.00
PAVF-C	L_∞^j	Error	1.174×10^{-2}	3.014×10^{-3}	7.527×10^{-4}
		Order	/	1.96	2.00
	L_2^j	Error	1.135×10^{-2}	4.371×10^{-3}	1.094×10^{-3}
		order	/	1.99	2.00
PAVF-P	L_∞^j	Error	7.501×10^{-3}	1.892×10^{-3}	4.730×10^{-4}
		Order	/	1.99	2.00
	L_2^j	Error	4.240×10^{-3}	1.122×10^{-3}	2.796×10^{-4}
		order	/	1.91	2.00

Table 2 lists the L_∞^n and L_2^n errors and convergence order in time. From the table, we see that all methods reach the second order in time except the PAVF method which is only first-order. From Table 1 and Table 2, we can see that the PAVF-P method has higher accuracy than the PAVF and PAVF-C methods. Table 3 and Figure 1 represent the CPU time of the four methods with different temporal steps. All computations were done on a custom computer with i7-1.80 GHz. To estimate how long a portion of our algorithm takes to run we used the Matlab stopwatch timer functions, tic and toc. The Matlab (R2024b) built-in functions tic and toc are used to measure the performance of the algorithms. These functions return wall-clock time. Since the PAVF method and the PAVF-C method are semi-implicit, they require a solution of two linear systems of equations as well as the solution of two nonlinear systems of equations. On the other hand, fully implicit PAVF-P and AVF methods require the solution of four nonlinear systems

Table 2. The L_∞^n and L_2^n errors and convergence orders in time of the proposed methods with $h = 0.01, -16 \le x \le 16$ at $t = 1$.

		τ	0.5	0.25	0.125
AVF [18]	L_∞^n	Error	2.889×10^{-3}	7.274×10^{-4}	1.845×10^{-4}
		Order	/	1.99	1.98
	L_2^n	Error	4.902×10^{-3}	1.243×10^{-3}	3.210×10^{-4}
		order	/	1.98	1.95
PAVF	L_∞^n	Error	1.966×10^{-2}	1.061×10^{-2}	5.393×10^{-3}
		Order	/	0.89	0.98
	L_2^n	Error	3.238×10^{-2}	1.725×10^{-2}	8.788×10^{-3}
		order	/	0.91	0.97
PAVF-C	L_∞^n	Error	2.078×10^{-3}	5.116×10^{-4}	1.285×10^{-4}
		Order	/	2.02	1.99
	L_2^n	Error	3.456×10^{-3}	8.685×10^{-4}	2.316×10^{-4}
		order	/	1.99	1.91
PAVF-P	L_∞^n	Error	2.086×10^{-3}	5.409×10^{-4}	1.397×10^{-4}
		Order	/	1.99	2.00
	L_2^n	Error	3.277×10^{-3}	8.441×10^{-4}	2.228×10^{-4}
		order	/	1.96	1.92

Table 3. Computation time for $-32 \le x \le 32$ at $t = 1$.

	PAVF		PAVF-C		PAVF-P		AVF [18]	
τ	$h = 0.1$	$h = 0.05$	$h = 0.1$	$h = 0.05$	$h = 0.1$	$h = 0.05$	$h = 0.1$	$h = 0.05$
0.1	0.083	0.137	0.129	0.239	0.165	0.350	0.249	0.405
0.05	0.121	0.240	0.217	0.263	0.220	0.479	0.240	0.509
0.01	0.509	1.138	0.994	2.206	0.987	2.087	1.097	2.218
0.005	1.002	3.123	2.027	6.132	1.995	5.528	2.026	4.590

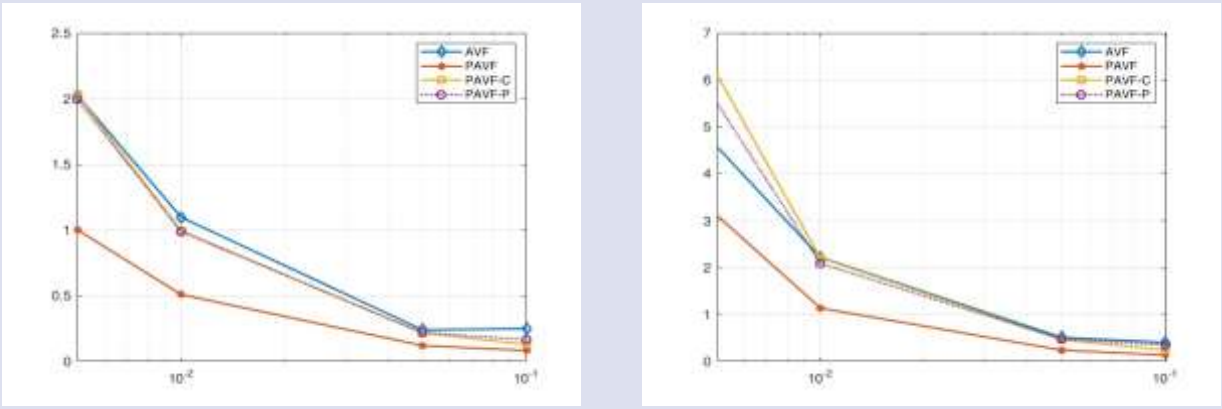

(a) h=0.1 (b) h=0.5

Figure 1. Computation time for -32≤x≤32 at t=1.

of equations. Accordingly, the PAVF method is more efficient than the AVF method. Figure 1 verifies this fact. Table 3 also shows that the computational costs of PAVF and PAVF-C are less than the fully implicit PAVF-P and AVF methods. In addition, we notice that the computational times of the PAVF-C and PAVF-P methods are slightly less than twice that of PAVF although the PAVF-C method is the composition of the PAVF method and its adjoint method, and the PAVF-P method is fully implicit. In addition, the PAVF-C and the PAVF-P methods have the same accuracy as the AVF method, but they are more efficient than the AVF method. Finally, we can say that the PAVF-P is the most efficient method.

Next, we test the stability of the scheme concerning the initial data. We consider the perturbed initial data $u_{noise}(x,0) = u_0(x)(1+\mu\theta), v_{noise}(x,0) = v_0(x)(1+\mu\theta), v_{t,noise}(x,0) = v_{t,0}(x)(1+\mu\theta)$, where μ is the percentage of the noise and θ is the random variable generated from a uniform distribution in the interval $[-0.5,0.5]$. We denote the perturbed solution as U_p and V_p. Figure 2 represents the solitary wave obtained by the PAVF scheme (28) with noise using the perturbed initial condition with $\mu = 0.2$. Similar results have been obtained for the PAVF-C and PAVF-P methods which are not shown here. From the figure, we see that the small perturbation in the initial data does not yield any significant effect on the wave propagation, which confirms the stability of the methods.

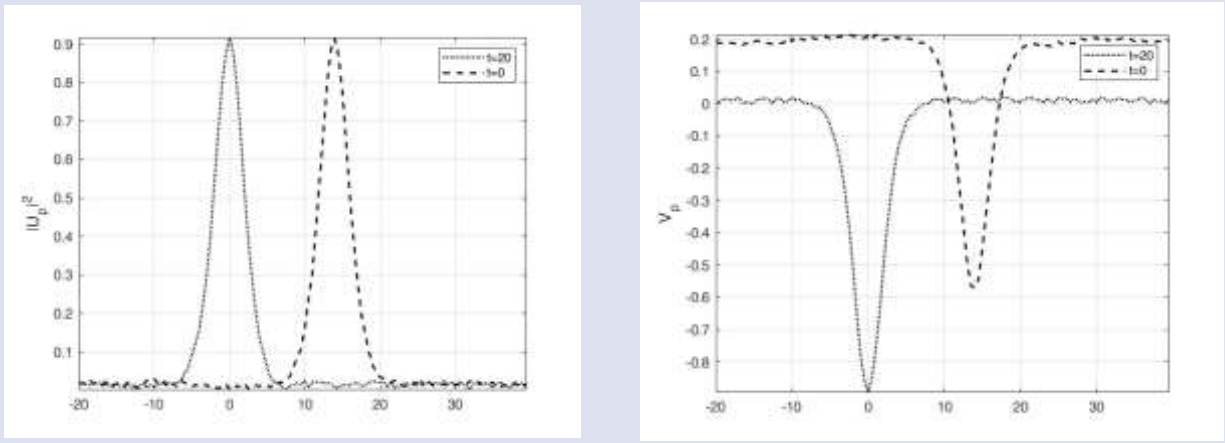

(a) h=0.1 (b) h=0.5

Figure 2. Solitary wave propagation with noise. τ=0.001,h=0.5.

Single solitary wave: In this subsection, we examine the long-time solitary wave simulation. We solve the SB equations (1) in the spatial interval $[-64,64]$ and temporal interval [0,40]. We choose the spatial interval large enough so that solitary wave propagation and conservation properties are not affected by the boundary conditions. We can see that solitons move forward without any changes in shape as shown in Fig.3. The corresponding errors of total energy H^n and mass M^n are represented by Fig.4. From the figure, we see that the errors are small during long-time integration which confirms theoretical results. Fig 3(a) represents that all four methods preserve the discrete energy up to round-off errors. From Fig. 3(b) we can see that, the AVF method cannot preserve the mass, but the relative error is bounded. On the other hand, we can see the excellent mass preservation of the other three methods during time integration.

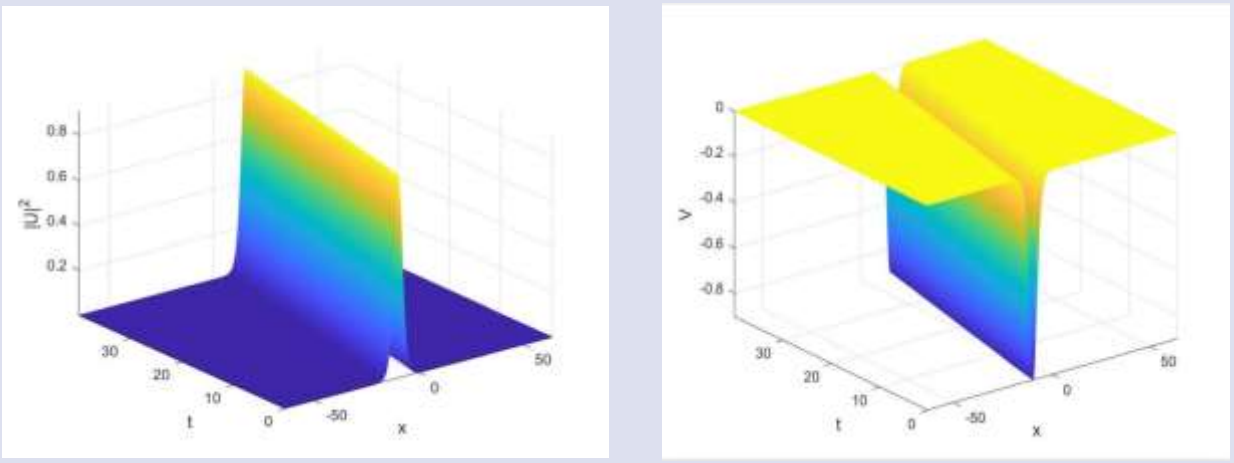

(a) h=0.1 (b) h=0.5

Figure 3. Evolution of PAVF solution for τ=0.001,h=0.2

Numerical results show that the proposed schemes have excellent conservation properties and stability even for long time integration.

Two-dimensional Schrodinger-Boussinesq equation

The advantage of the PAVF method becomes more evident in two-dimensional problems [16]. In this subsection, we consider the two-dimensional SB equations (1) with $d = 2$, and $f(v) = \sin(v)$ [19,20]. We choose the parameters

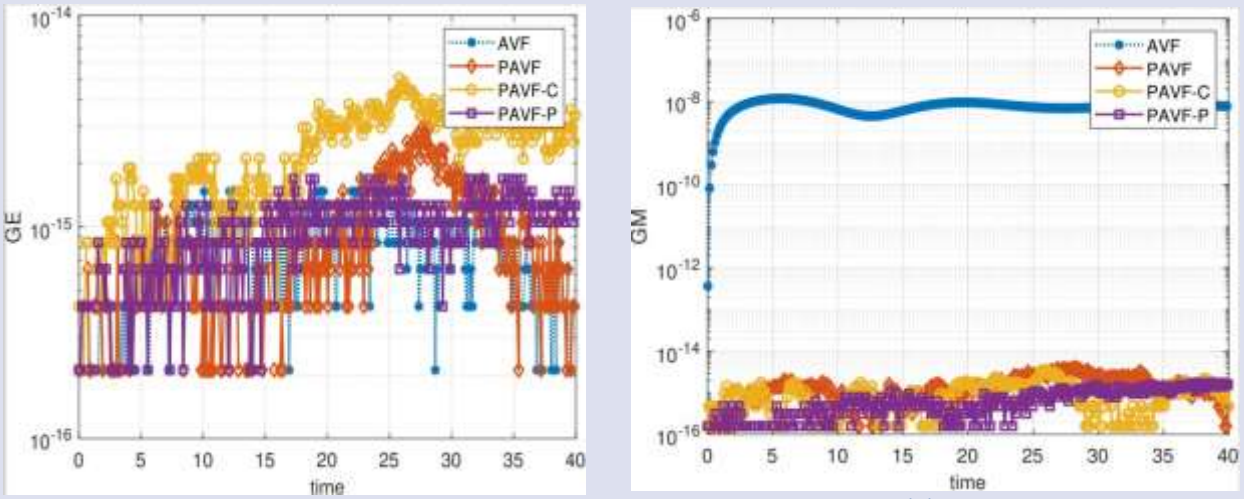

(a) h=0.1 (b) h=0.5

Figure 4. Relative errors in total energy H^n and the mass M^n for τ=0.01,h=0.2.

Table 4. Computation time for $h_x = h_y = 0.25, -10 \le x, y \le 10$ at $t = 1$.

τ	PAVF	PAVF-C	PAVF-P	AVF [18]
0.1	3.609	6.575	13.794	8.552
0.05	5.160	9.670	18.047	15.798
0.01	28.731	57.022	97.931	66.328
0.005	58.076	116.404	200.128	131.089

$\gamma = \alpha = -1$ and $\xi = \omega = -1/10$. The analytical solution of two-dimensional SB equation is not available. The initial data are taken as [19]

$$u_0(x,y) = \frac{2}{e^{x^2+2y^2} + e^{-(x^2+2y^2)}} e^{5i/\cosh(\sqrt{4x^2+y^2})}$$
$$v_0(x,y) = e^{-(x^2+2y^2)}$$
$$\phi_0(x,y) = \frac{1}{2} e^{-(x^2+2y^2)} \quad (38)$$

Table 4 indicates the computational time obtained by four energy-preserving methods in the spatial domain $\Omega = (-10 \times 10) \times (-10 \times 10)$ with $h_x = h_y = 0.1$ for the different temporal step size. Here, h_x and h_y are step size in x −direction and y −direction, respectively. From the table, we see the PAVF method requires smaller computational time than the AVF method, as expected. Moreover, as in the one-dimensional case, the computational time of PAVF-C method is much less than twice that of PAVF. In addition, it can be seen that the PAVF-P method is a method with the most CPU time.

Fig. 5 shows the surfaces of $|u|, v$ and ϕ at the initial time $t = 0$ and the final time $t = 1$. The spatial interval is set to $\Omega = [-16 \times 16] \times [-16 \times 16]$. The step sizes are taken as $\tau = 0.01$ and $h_x = h_y = 0.25$.

From the left plot of the figure, one can see the initial hump collapses as time evolves many spikes appear at the end. From the middle plot, one can see that the initial hump collapses as time evolves, and a hole appears inside the hump. In addition, there are spikes from under the horizontal plane. The right graph displays the evolution of the plane ϕ. From the right figure, one can see that again the initial hump collapses, but no hole appears. Moreover, spikes from under the horizontal plane. The energy and mass conservations are depicted in Fig.6. From the figure, one can find that PAVF-C preserves the total energy better than the other methods. Moreover, all PAVF methods preserve the mass better than the AVF method.

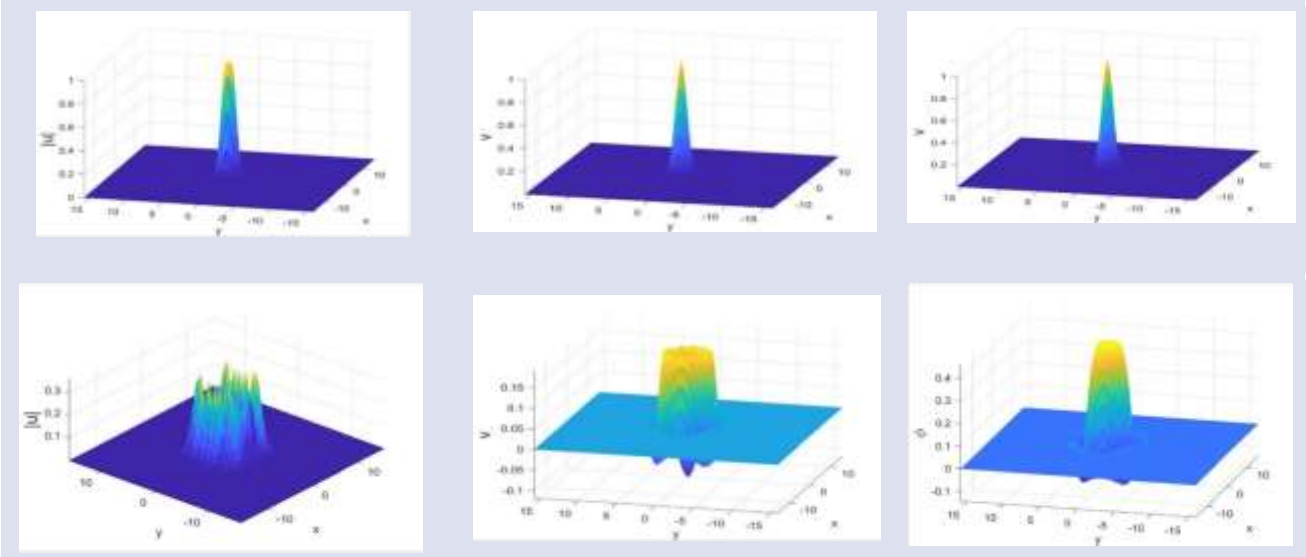

Figure 5. Evolution of PAVF solution for τ=0.01,h_x=h_y=0.25

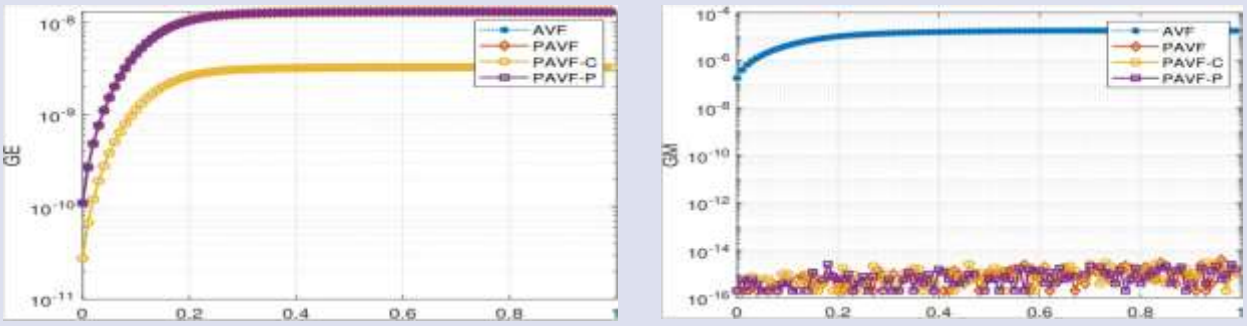

Figure 6. Error in the total energy H^n and the mass L^n for τ=0.01,h=0.25.

Conclusion

In this study, we applied the energy-preserving PAVF method to the one-dimensional and two-dimensional CNSB equations. The method leads to semi-implicit algebraic equations for the CNSB equations. In addition, we find that the new energy-preserving scheme preserves the mass of the equations. In conjunction with the adjoint method of the PAVF method, we further introduce the conservative PAVF composition (PAVF-C) method and (PAVF-P) method. Some numerical results are presented to demonstrate the accuracy and efficiency of the method for the numerical solution of the CNSB equations. Numerical results confirm the theoretical results. Errors in the methods and computational times are compared with the AVF method. Numerical results verify that the applied schemes simulate both one- and two-dimensional CNSB system well.

Conflict of interest

There are no conflicts of interest in this work.

Acknowledgments

The authors' gratitude to the reviewers for their valuable contributions.

References

[1] Zhang H., Song S.H., Chen X.D., Zhou W.E., Average vector field methods for the coupled Schrödinger—KdV equations, *Chinese Physics B*, 23(7) (2014) 070208.

[2] Aydın A., Multisymplectic integration of N-coupled nonlinear Schrödinger equation with destabilized periodic wave solutions, *Chaos, Solitons & Fractals*, 41(2) (2009) 735-751.

[3] Wang L., Wang Y., Multisymplectic structure-preserving scheme for the coupled Gross–Pitaevskii equations, *International Journal of Computer Mathematics*, 98(4) (2021) 783-806.

[4] Yajima N., Satsuma J., Soliton solutions in a diatomic lattice system, *Progress of Theoretical Physics*, 62(2) (1979) 370-378.

[5] Rao N.N., Coupled scalar field equations for nonlinear wave modulations in dispersive media, *Pramana*, 46 (1996) 161-202.

[6] Huang L.Y., Jiao Y.D., Liang D.M., Multi-symplectic scheme for the coupled Schrödinger—Boussinesq equations, *Chinese Physics B*, 22(7) (2013) 070201.

[7] Bai D., Zhang L., The quadratic B-spline finite-element method for the coupled Schrödinger–Boussinesq equations, *International Journal of Computer Mathematics*, 88(8) (2011) 1714-1729.

[8] Zhang L., Bai D., Wang S., Numerical analysis for a conservative difference scheme to solve the Schrödinger–Boussinesq equation, *Journal of computational and applied mathematics*, 235(17) (2011) 4899-4915.

[9] Fei Z., Pérez-García V.M., Vázquez L., Numerical simulation of nonlinear Schrödinger systems: a new conservative scheme, *Applied Mathematics and Computation*, 71(2-3) (1995) 165-177.

[10] Bai D., Wang J., The time-splitting Fourier spectral method for the coupled Schrödinger–Boussinesq equations. *Communications in Nonlinear Science and Numerical Simulation*, 17(3) (2012) 1201-1210.

[11] Liao F., Zhang L., Wang S., Time-splitting combined with exponential wave integrator Fourier pseudospectral method for Schrödinger–Boussinesq system, *Communications in Nonlinear Science and Numerical Simulation*, 55 (2018) 93-104.

[12] Hairer E., Wanner G., Lubich C., Hairer E., Wanner G., Lubich C., Symmetric Integration and Reversibility, *Geometric Numerical Integration: Structure-Preserving Algorithms for Ordinary Differential Equations*, (2006) 143-178.

[13] Quispel G.R.W., McLaren D.I., A new class of energy-preserving numerical integration methods, *Journal of Physics A: Mathematical and Theoretical*, 41(4) (2008) 045206.

[14] Celledoni E., Grimm V., McLachlan R.I., McLaren D.I., O'Neale D., Owren B. and Quispel G.R.W., Preserving energy resp. dissipation in numerical PDEs using the "Average Vector Field" method, *Journal of Computational Physics*, 231(20) (2012) 6770-6789.

[15] Wang L., Cai W., Wang Y., An energy-preserving scheme for the coupled Gross-Pitaevskii equations, *Adv. Appl. Math. Mech.*, 13(1) (2021) 203-231.

[16] Cai W., Li H., Wang Y., Partitioned averaged vector field methods. *Journal of Computational Physics*, 370 (2018) 25-42.

[17] Wang J., Conservative Fourier spectral scheme for the coupled Schrödinger–Boussinesq equations, *Advances in Difference Equations*, (2018) 1-19.

[18] Aydin A, Mohammed T.Y., An Energy Preserving Scheme for CSB System, 2^{nd} Int. Grad. Stud.Cong. (IGSCONG-22), Proceeding Book, ISBN: 978-605-73639-2-3, 91-101.

[19] Cai J., Chen J., Yang B., Efficient energy-preserving wavelet collocation schemes for the coupled nonlinear Schrödinger-Boussinesq system, *Applied Mathematics and Computation*, 357 (2019) 1-11.

[20] Liao F., Zhang L., Conservative compact finite difference scheme for the coupled S chrödinger–B oussinesq equation, *Numerical Methods for Partial Differential Equations*, 32(6) (2016) 1667-1688.

[21] Aydın A., Karasözen B., Lobatto IIIA–IIIB discretization of the strongly coupled nonlinear Schrödinger equation, *Journal of computational and applied mathematics*, 235(16) (2011) 4770-4779.

[22] Aydın A., Karasözen B., Symplectic and multi-symplectic methods for coupled nonlinear Schrödinger equations with periodic solutions, *Computer Physics Communications*, *177*(7) (2007) 566-583.

[23] Leimkuhler B., Reich S., Simulating Hamiltonian dynamics (No. 14). Cambridge University Press, (2004)

[24] Aydin, A., Sabawe, BAK., New conservative schemes for Zakharov equation, *Turk. J. Math. Comput. Sci.* 15(2) (2023) 227-293.

[25] Ismail M. S., Ashi H. A., A compact finite difference scheme for solving the coupled nonlinear Schrodinger-Boussinesq equations, *Applied Mathematics* , 7 (2016) 605-615.

[26] Hu X., Wang S., Zhang L., Maximum error estimates for a compact difference scheme of the coupled nonlinear Schrödinger–Boussinesq equations, *Numerical Methods for Partial Differential Equations,* 35(6) (2019) 1971-1999.

[27] Deng D., Wu Q., Analysis of the linearly energy-and mass-preserving finite difference methods for the coupled Schrödinger-Boussinesq equations, *Applied Numerical Mathematics,* 170 (2021) 14-38.

[28] Tingchun W., Boling G., Qiubin X., Fourth-order compact and energy conservative difference schemes for the nonlinear Schrödinger equation in two dimensions, *Journal of Computational Physics,* 243 (2013) 382–399.

[29] Hong-Lin L., Zhi-Zhong S., Han-Sheng S., Error Estimate of Fourth-Order Compact Scheme For Linear Schrödinger Equations, *SIAM J. Numer. Anal.,* 47(6) (2010) 4381–4401.

[30] Gholamreza K., Hadi MF., The Matrix Transformation Technique for the Time-Space Fractional Linear Schrödinger Equation, *Iranian Journal of Mathematical Chemistry,* 15(3) (2024) 137-154.

[31] Gholamreza K., Hadi MF., Unconditionally stable finite element method for the variable-order fractional Schrödinger equation with Mittag-Leffler kernel, *Journal of Mathematical Modeling*, 12(3) (2024) 533–550.